THE JOURNAL OF PHYSICAL CHEMISTRY B

Article

Cite This: J. Phys. Chem. B 2019, 123, 8838−8847

pubs.acs.org/JPCB

Coil−Globule Transition Thermodynamics of Poly(*N*-isopropylacrylamide)

Maren Podewitz,[‡] Yin Wang,[‡] Patrick K. Quoika, Johannes R. Loeffler, Michael Schauperl,[†] and Klaus R. Liedl*

Institute of General, Inorganic and Theoretical Chemistry, and Center for Molecular Biosciences Innsbruck (CMBI), University of Innsbruck, Innrain 80-82, A-6020 Innsbruck, Austria

Supporting Information

ABSTRACT: Thermosensitive polymers such as poly(*N*-isopropylacrylamide) (PNIPAM) undergo a phase transition in aqueous solution from a random-coil structural ensemble to a globule structural ensemble at the lower critical solution temperature (LCST). Above this temperature, PNIPAM agglomerates and becomes insoluble, whereas it is soluble below the temperature. Thus, thermosensitive polymers represent essential targets for several applications, e.g., in drug delivery. Although their ability to change structure in response to a temperature alteration is highly relevant for industrial processes, their thermodynamic properties are mostly qualitatively understood, and the quantitative thermodynamic picture is still elusive. In this study, we used a combined atomistic molecular dynamics and well-tempered metadynamics simulation approach to estimate coil−globule transition thermodynamics. An isotactic 30-mer of PNIPAM was investigated over a broad temperature range between 200 and 360 K. The transition from the globule to the random-coil structure was observed with well-tempered metadynamics. For the first time, the free energy surface of PNIPAM was estimated and it is shown that the simulation results are in line with the experimentally observed thermosensitive behavior. Below the LCST, the random-coil ensemble represents the global energy minimum and is thermodynamically favored by 21 ± 9 kJ/mol compared to the globule ensemble; both are separated by a barrier of 49 ± 14 kJ/mol. In contrast, above the LCST, the globule ensemble is thermodynamically favored by 21 ± 8 kJ/mol over the random-coil ensemble. The barrier from random-coil to globule is 17 ± 10 kJ/mol.

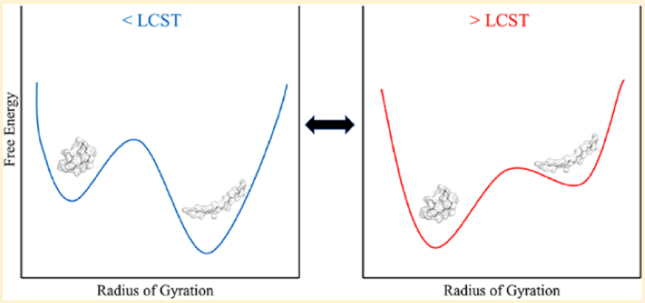

1. INTRODUCTION

Poly(*N*-isopropylacrylamide) (PNIPAM) is a thermosensitive polymer with a lower critical solution temperature (LCST) of 305 K in aqueous solution.[1] Below the LCST, PNIPAM is soluble in water whereas, above the LCST, the well-solvated random-coil conformation of PNIPAM collapses into globule conformations, aggregates subsequently, and eventually becomes insoluble.[2] Since the coil−globule conformational transition is strongly linked to phase separation, we use the LCST to describe the conformational transition temperature. This temperature-sensitive feature gives PNIPAM potential for biomedical applications[3−10] such as drug delivery[11−16] and biomolecular imaging.[17] Engineering the LCST of PNIPAM is an active field of research. It can be achieved by (i) variation of the chain length,[18,19] (ii) introducing hydrophilic monomer units, e.g., *N*,*N*-dimethylacrylamide or other acrylamides to get a copolymer,[20,21] (iii) altering the polymer tacticity,[21−24] (iv) adding hydrated ions,[25,26] urea,[27,28] or cosolvents,[29−35] or (v) applying pressure.[36]

The phase transition mechanism and the physicochemical properties of the PNIPAM have extensively been studied both experimentally[37−49] and theoretically.[19,36,50−63] Experimental studies suggest that below the LCST, the amide of the side chain is fully exposed to water in the extended random-coil conformation. The PNIPAM surrounding water molecules create a solvation shell and stabilize the extended polymer structure by hydrogen bonds.[40] As temperature increases above the LCST, it is believed that during the coil−globule transition, the increasing entropy of the water molecules at the isopropyl groups causes a polymer collapse, such that the polymer's hydrophobic surface is minimized.[40,41,51−53] Studies suggest that the water molecules that were hydrogen-bonded to amide groups are squeezed out due to the collapse, which results in a decreasing hydration number, i.e., fewer solute−solvent hydrogen bonds.[41,42,50,60] Futscher et al. pointed out the importance of hydration changes in the polymer backbone during this process.[43] Eventually, PNIPAM adopts a globule-like conformation in aqueous solution. The coil−globule transition mechanism is backed up by theoretical studies, which found the surrounding water arrangement to become unstable and the hydrophobic interactions to become dominant above the LCST.[51−53] In addition, Kang et al.

Received: June 27, 2019
Revised: September 23, 2019
Published: September 23, 2019

DOI: 10.1021/acs.jpcb.9b06125
J. Phys. Chem. B 2019, 123, 8838−8847

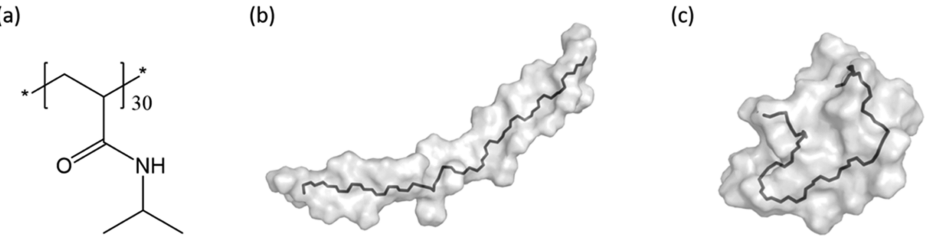

Figure 1. (a) 30-mer poly(*N*-isopropylacrylamide) in (b) random-coil and (c) globule conformation. The two representative structures were randomly picked from our simulations.

suggested that strong intramolecular hydrogen bonds are formed in the globule resulting in further stabilization,[55] whereas, Tavagnacco et al. showed that methyl rotations and PNIPAM−water interactions are crucial in maintaining a random-coil conformation.[61] All of these studies provide valuable insights into the phase transition mechanism. However, as pointed out by Kang et al. and others, very long simulation times (>1 μs) are necessary to provide a reliable description of the system.[54,55,64]

Pioneered by Dalgicdir et al.,[65,66] the PNIPAM coil−globule transition thermodynamics were calculated using molecular dynamics (MD) simulations. While the free energy of hydration and free energy of solvation of the monomer NIPAM were characterized,[67] to our knowledge, there is no computational study that presents the free energy surface of PNIPAM in dependence of the radius of gyration (ROG) above and below the LCST. In fact, no study exists that shows that the used force fields can reproduce the experimental behavior by quantitative comparison of the free energies of the coil versus globule ensembles: below the LCST the random-coil structural ensemble is thermodynamically favored (lower free energy ΔG), whereas, above the LCST, the globule ensemble is favored. Adequate sampling of PNIPAM, especially in the globule ensemble, is challenging due to its huge conformational space. Different sampling approaches, such as large-scale conformational sampling[65,66,68] and the adaptive biasing force method,[67] were used in previous studies. While it is known that aggregation between multiple polymer chains plays a role,[46,54] the correct thermosensitive behavior was experimentally also found for a single chain.[69]

While in experiments[70,71] (and many computational studies[19,21,51]), PNIPAM is characterized in terms of the radius of gyration (ROG), it is essential to note that a specific ROG does not correspond to one well-defined structure but rather to a large ensemble of different conformations. Unlike proteins that exhibit a well-defined fold, no such well-defined globule conformation is found for PNIPAM. Instead, it collapses to diverse globule conformations. While having a similar ROG, each structure of the globule ensemble may vary in its root-mean-square deviation (RMSD) and in its molecular conformation, as also discussed in the literature,[55,65,66,68] where they distinguish between two major globule conformations. This diversity has to be taken into account when analyzing the thermodynamics and we will refer to the globule state as the globule conformational ensemble.

In this study, we report the potential free energy surfaces of an isotactic 30-mer of PNIPAM above and below the LCST, and show that the OPLS2005 force field[72,73] agrees with the experimentally observed thermosensitive behavior. Simulations of a 30-mer of PNIPAM over a temperature range from 200 to 360 K were performed to determine the LCST for the given force field with a simulation time of 1 μs for each temperature. For temperatures close to the phase transition temperature, 2 μs was simulated to account for the slow relaxation time of PNIPAM.[54,55] Random-coil structures stayed at random-coil conformations at temperatures below the LCST, and spontaneous coil−globule transitions were observed for temperatures above the LCST. To enforce swelling below the LCST and to sample the random-coil ensemble above the LCST, well-tempered metadynamics simulations were performed. To cover the vast conformational space of the globule ensemble of PNIPAM,[55] we randomly selected 40 different globule structures from our free MD simulations.

2. METHODS

2.1. Simulation Setup. The polymer we studied was a 30-mer poly(*N*-isopropylacrylamide) (Figure 1a) chain with both ends terminated with hydrogen atoms. The monomers were arranged on the same side of the main chain (15R-14S) and resulted in a fully isotactic arrangement. The chosen length of 30 repeating units in the polymer ensured a realistic and computationally still trackable model with acceptable simulation cost, in particular, because for very short oligomers no or a much lower LCST is observed.[19,50,51] Based on the ROG, two conformational ensembles of the polymer can be distinguished: a compact globule conformational ensemble with a small ROG, typically <1.2 nm, and a random-coil conformational ensemble with a ROG of >1.6 nm. We want to stress here that many different molecular conformations of PNIPAM have the same ROG but may differ in their RMSDs. Nevertheless, Figure 1 shows two random individual structures, one in an extended random-coil conformation (Figure 1b) and another in a globule conformation (Figure 1c).

To start our simulations, we prepared a random-coil polymer structure using Maestro[74] and placed it in the center of an 8 × 8 × 8 nm^3 simulation box filled with extended simple point-charge (SPC/E)[75] water. The periodic boundary condition was applied to each dimension. The OPLS2005 force field[72,73] was chosen for PNIPAM because it was reported to most adequately reproduce the lower critical solution temperature (LCST) compared to all tested combinations of force fields/water models.[76]

We used GROMACS 2016.4[77,78] in all simulations with a time step of 2 fs, and the trajectory was saved every 20 ps. The linear constraint solver[79] was applied to bonds containing hydrogen atoms. The short-range electrostatic and the van der Waals cutoff were both set to 1 nm, and fast smooth particle mesh Ewald[80] electrostatics were used for long-range electrostatic interactions. Simulations were carried out in the NpT ensemble at 1 bar with temperature coupling using velocity

DOI: 10.1021/acs.jpcb.9b06125
J. Phys. Chem. B 2019, 123, 8838−8847

rescaling[81] and pressure coupling using the Parrinello–Rahman method.[82]

The random-coil polymer mentioned before was energy-minimized using the steepest descent algorithm. The minimized conformation was used as a starting structure to investigate the coil–globule transition and the LCST. A snapshot of the starting structure and the backbone dihedral distribution can be found in Figure S1. The starting structure was simulated at different temperatures from 200 to 360 K with a temperature step of 10 K and 1 μs for each temperature. To get a more precise LCST, existing simulations at temperatures close to the LCST were extended and additional simulations were performed. In total, we simulated at 20 different temperatures summing up to 26 μs. Detailed simulation lengths and temperatures are shown in Figure S2. The radius of gyration (ROG) and the solvent-accessible surface area[83] (SASA) were calculated using the GROMACS built-in tools. A solvent probe with a radius of 0.14 nm was used for calculating the SASA. For each simulation, the first 250 ns were discarded.

2.2. Well-Tempered Metadynamics Simulation Setup. All free MD simulation trajectories summing up to 26 μs were projected into the conformational space of ROG versus SASA. In the histograms of ROG and SASA, there were two distinct peaks. Large SASA and ROG values suggest random-coil conformations, whereas globule conformations feature small SASA and ROG values. The minimum population positions of the histogram of SASA and ROG are considered to be the borders of the bimodal distribution separating the random-coil from the globule conformational ensemble. Forty globule structures with a SASA smaller than 38.75 nm^2 and ROG smaller than 1.225 nm were selected randomly from the simulation trajectories at temperatures above the force field LCST, from 270 to 360 K with a step of 10 K. In these 10 simulation trajectories, only the first 1000 ns were used for consistency. The 40 globule structures were then used as the starting structures for the well-tempered metadynamics simulations.

In metadynamics simulations, history-dependent Gaussian shape potentials were added to impel the system to escape local minima.[84] In the well-tempered variant of metadynamics, the height of the Gaussian potential decreases with simulation time.[85] We used GROMACS 2016.4 with the PLUMED 2.4.0 plugin[86] and performed well-tempered metadynamics simulations to enforce the swelling of the polymer and ultimately to obtain the free energy surface above and below the LCST. The ROG was chosen as the collective variable. The initial height of the Gaussian function was set to 3.5 kJ/mol and the width was set to 0.35 nm, with a bias factor of 10. The values of the collective variable and the metadynamics bias potential were stored every 10 steps.

Spontaneous coil–globule transitions at high temperature have already been observed in free simulations.[51] Thus, we focus on globule–coil transitions at low temperature. Hence, we started metadynamics simulations from globule conformations only.

Each of the 40 globule structures was simulated for 1000 ns at 250 and 300 K, i.e., above and below the force field's LCST. We reweighted[87] and reconstructed the 40 individual free energy surfaces at 250 and 300 K from the simulation results using the method published by Tiwary and Parrinello.[88] The 40 individual surfaces were averaged for each temperature separately to obtain the average of the free energy surfaces above and below the LCST. Results were validated using the leave-one-out cross-validation.

Furthermore, we combined the multitude of metadynamics simulations with respect to their underlying probability distributions. Assuming all starting structures to be equally probable, we used their free energies as references. Therefore, we subtracted the respective value of the free energy of the starting structure, that is, setting the energy of the ROG bin that contains the starting structure to zero, before transforming the free energy curve of every simulation to a corresponding probability distribution. Thus, we obtained the ratio of probabilities relative to the respective starting structure. After the transformation, we added up the probability ratios of the individual simulations with respect to binned values of radius of gyration. We normalized our obtained combined probability distribution before we performed a Boltzmann inversion to obtain a combined free energy surface. We declared a range of uncertainty from leave-one-out validation runs, by indicating the highest deviations from the combined curve in directions of both, higher and lower free energies.

The reaction rate constant k, half-life period $t_{1/2}$, and equilibrium constant K_{equ} can be calculated according to the following equations

$$k = \frac{k_B T}{h} e^{-\Delta G^*/RT} \quad (1)$$

$$t_{1/2} = \frac{\ln 2}{k} \approx \frac{0.693}{k} \quad (2)$$

$$K_{equ} = e^{-\Delta G^{250}/RT} \quad (3)$$

where k_B is the Boltzmann's constant, h is the Planck's constant, R is the gas constant, T is the temperature, ΔG^* is the free energy barrier, and ΔG^{250} (ΔG^{300}) is the free energy difference of the two conformational states at 250 K (300 K).

3. RESULTS

3.1. Sampling of Transitions. *3.1.1. Coil–Globule Transition.* To sample the transition from the random-coil to the globule ensemble, we simulated the behavior of an isotactic 30-mer of PNIPAM between 200 and 360 K for up to 2 μs for each temperature. The average and standard deviation of the ROG and the SASA versus temperature are shown in Figure 2. For temperatures below 260 K, the ROG—depicted in black in Figure 2—remains at large values at around 1.7 nm and the SASA—depicted in red in Figure 2—around 43 nm^2, which indicates that the polymers stay in a random-coil conformation over the whole simulation time. At temperatures of 280 K and above, the averaged ROG is around 1.0 nm and the SASA drops down to 33 nm^2, which is indicative of a globule conformation. Between 260 and 280 K, a rapid decay in the ROG and SASA is observed accompanied by large standard deviations as indicated by the black and red bars. From Figure 2, it is clear that the coil–globule transition occurs between 260 and 280 K.

Looking at the individual simulations at various temperatures, depicted in the Supporting Information in Figure S5, one may see from the ROG versus time plots that above 267.5 K, a spontaneous collapse to the globule conformation was observed indicated by a drop in ROG from 1.7 nm to around 1.0 nm. One may also see that at 270 K, it took more than 1500 ns for the coil–globule transition to occur. It still took

DOI: 10.1021/acs.jpcb.9b06125
J. Phys. Chem. B 2019, 123, 8838–8847

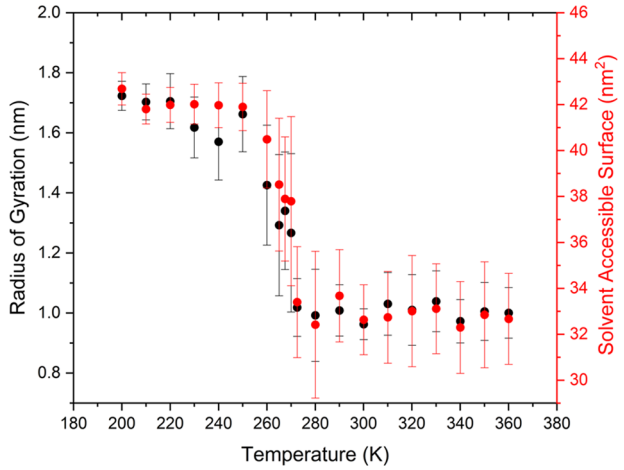

Figure 2. Average and standard deviation of the radius of gyration (ROG) in nm (left axis: depicted in black) and the solvent-accessible surface area (SASA) in nm^2 (right axis: depicted in red) vs temperature plot for an isotactic PNIPAM 30-mer. A coil−globule transition is found between 260 and 280 K.

almost 1000 ns at 272.5 K and this time decreased to 500 ns at 280 K, and to 250 ns at 290, 300, and 310 K. For even higher temperatures, the coil−globule transition happened almost instantaneously, suggesting that it is thermodynamically favored at these conditions. For temperatures in the phase transition zone, at 260, 265, and 267.5 K, the ROG versus time plots show oscillations in the ROG suggesting that the polymer switches between random-coil and globule conformations during simulations. It is worth noting that the experimental lower critical solution temperature transition of PNIPAM in water is 305 K.[1] Thus, we do have an offset between the calculated and experimental LCST of 30−40 K due to the force field.

When combining all trajectories obtained for the 20 simulations at temperatures between 200 and 360 K and projecting the structures in ROG versus SASA space, Figure 3 is obtained, where the axes depict the histograms of the ROG and the SASA populations. Clearly, the histograms show a bimodal distribution of PNIPAM structures, separated by a minimum at 1.225 nm for the ROG and 38.75 nm^2 for the SASA. Below these values, we find the globule state whereas above these values the random-coil state is located. From the two-dimensional (2D) conformational space depicted in Figure 3, it is clearly visible that the "globule state" does not correspond to a single molecular conformation but structures with a specific ROG can have quite a different SASA and may also differ in their RMSD values. Thus, we refer to the globule state as a globule conformational ensemble because it comprises a plethora of molecular PNIPAM conformations with similar ROG.

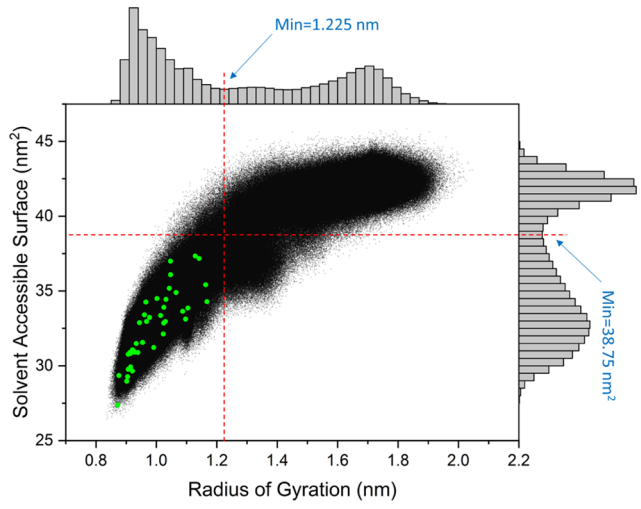

Figure 3. Simulation trajectories of all temperatures projected into the conformational space of the radius of gyration (ROG) vs the solvent-accessible surface area (SASA). The histograms of the ROG and the SASA are shown on the edges of the axes. Green points represent structures randomly selected for metadynamics simulations (vide infra).

The contributions of each simulation to this phase space are depicted in Figure S4 in the Supporting Information, where the ROG versus the SASA plots are depicted. At temperatures below the LCST, all sampled structures show large ROG and large SASA values suggesting random-coil conformations throughout the entire simulations. Similarly, at high temperatures, with a random-coil starting structure, the PNIPAM collapsed into a globule conformation and stayed there for the rest of the simulation time. However, for simulations at temperatures close to the force field LCST, the trajectories cover a large conformational space across random-coil and globule conformations.

3.1.2. Globule−Coil Transition. We observed the coil−globule transition at high temperatures and found that PNIPAM stayed at random-coil conformation at low temperatures when using the random-coil conformation as starting structure. We observed collapse and expansion in the temperature range of the coil−globule transition. However, when we simulated globule ensembles at low temperatures, we did not see a spontaneous swelling corresponding to a globule−coil transition. Instead, the globule ensembles were stable over the whole simulations. This finding is inconsistent with experimental results as we know the transition should be reversible.[1] However, at low temperatures, the systems may be kinetically trapped in a local minimum separated from the global minimum by a high energy barrier. The thermal energy may not be sufficient to overcome the barrier in the time scale of our simulations. To resolve this issue, we performed enhanced sampling, namely we used well-tempered metadynamics to sample the swelling of the globule structural ensemble, choosing the ROG as a collective variable to enforce expansion of PNIPAM and the globule to random-coil transition.

3.2. Sampling of the Globule Conformational Space.

The globule conformational space of PNIPAM is typically only characterized in terms of the ROG and the SASA. However, two globule PNIPAM conformations may have similar or the same values in ROG and SASA, yet they could be structurally very different. These individual conformations may also have very different globule to random-coil barriers. To address this sampling issue, we randomly picked 40 different globule starting structures from the globule conformational ensemble depicted in Figure 3. Selected structures, as indicated by green dots, were then subjected to metadynamics simulations. However, we are well aware that this does not result in a comprehensive sampling of the globule conformational space, which still is completely out of reach with current computational resources. Nevertheless, our approach provides a first reasonable estimate for the globule conformational space.

DOI: 10.1021/acs.jpcb.9b06125
J. Phys. Chem. B 2019, 123, 8838−8847

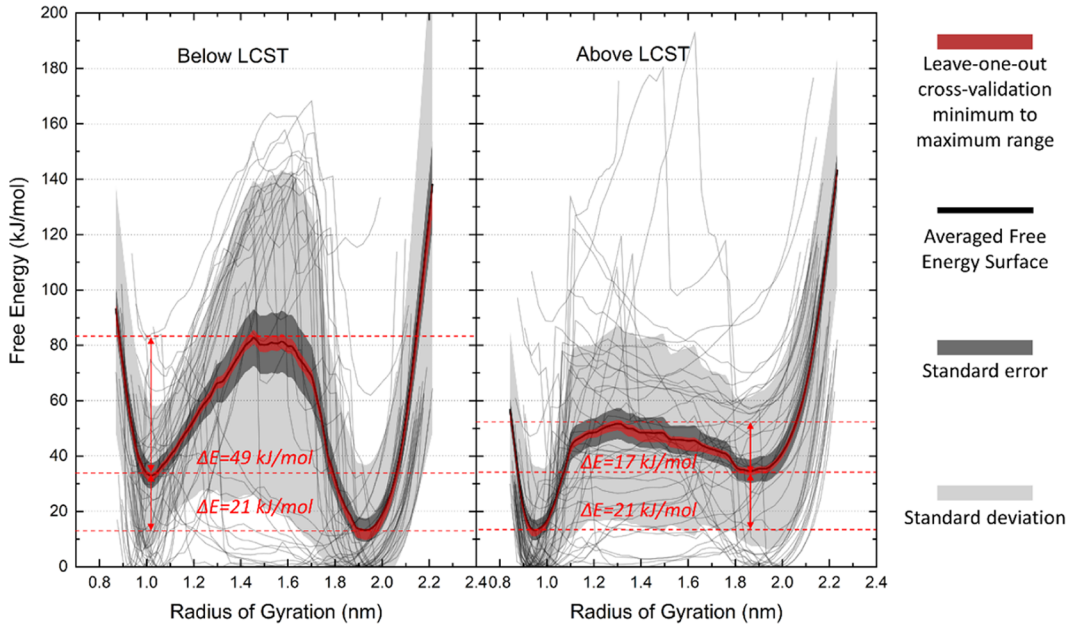

Figure 4. Averaged free energy surfaces of isotactic PNIPAM per oligomer vs radius of gyration from 40 metadynamics simulations below the force field LCST (250 K) and 40 metadynamics simulations above the force field LCST (300 K). The red band shows the minimum and maximum leave-one-out cross-validation range. Dark gray is the standard error of the averaged curves; light gray shows the standard deviation of the averaged curves. Light gray lines are the individual results of the 40 systems.

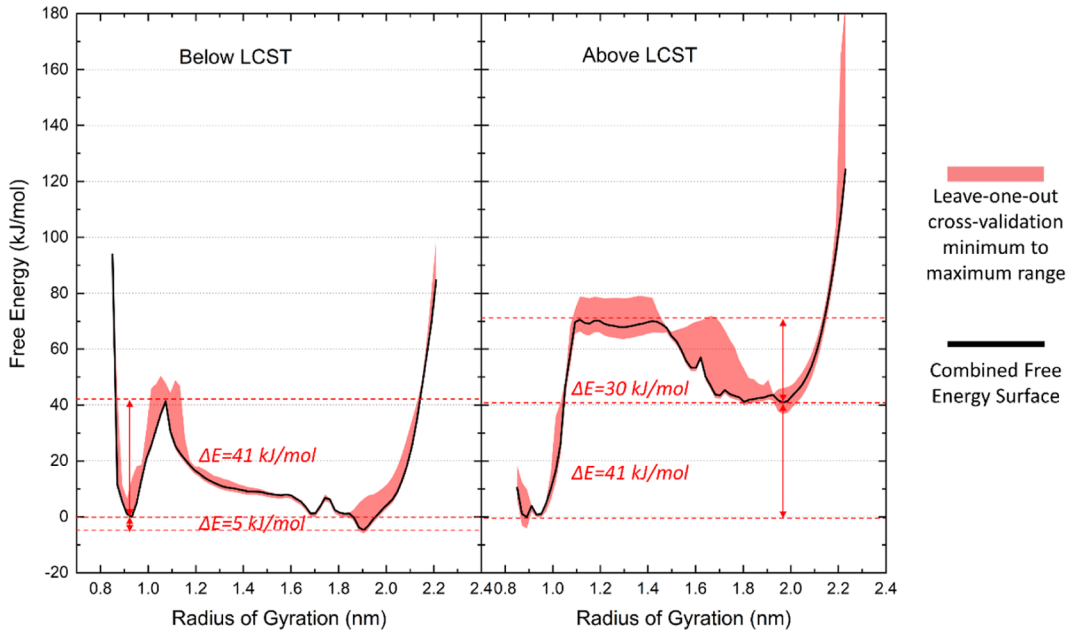

Figure 5. Combined free energy surfaces of isotactic PNIPAM per oligomer vs the radius of gyration from 40 metadynamics simulations below the force field LCST (250 K) and from 40 metadynamics simulations above the force field LCST (300 K). The red band depicts the minimum and maximum leave-one-out cross-validation range.

3.3. Free Energy Surfaces above and below the LCST.

To obtain the free energy surfaces above and below the LCST, we performed 40 well-tempered metadynamics simulations both at 250 and 300 K, which are above and below the force field's transition temperature starting from 40 distinct randomly drawn globule conformations. Each of these 80 simulations was run for 1000 ns and reweighted individually resulting in 2 × 40 surfaces. These were averaged to obtain estimates of the free energy surfaces of the two conformational ensembles depicted in Figure 4, where the averaged free energy is plotted against the ROG. The standard deviation is depicted in light gray and the standard error is depicted in dark gray. The resulting averaged free energy surfaces for each temperature are depicted in bold black lines, whereas the reweighted free energy surfaces of each individual system are shown as gray lines in the background.

At 250 K, the random-coil structure with a ROG around 1.9 nm is the thermodynamically preferred conformation favored by 21 ± 9 kJ/mol (standard error) over a globule conformation. The two structural ensembles are separated by

DOI: 10.1021/acs.jpcb.9b06125
J. Phys. Chem. B 2019, 123, 8838−8847

a barrier of 49 ± 14 kJ/mol, which needs to be overcome to reach the random-coil ensemble. At 300 K, the globule conformational ensemble with a ROG around 1.0 nm becomes the thermodynamically favored structure. It is by 21 ± 8 kJ/mol lower in free energy than the random-coil ensemble. The energy well of the random-coil conformation is quite shallow and the barrier to the globule ensemble is only 17 ± 10 kJ/mol. At 300 K, the globule ensemble has a narrow and deep free energy minimum in terms of ROG, whereas the random-coil has a somewhat broader not so pronounced minimum.

To test our results for stability, we calculated the minimum and maximum values in the leave-one-out cross-validation in addition to the average as indicated by a broad red curve in Figure 4. However, the minimum and maximum are very close to the average. These results indicate that no single curve dominates the average. It can be seen that the standard deviation (light gray) is quite significant, showing that different globule starting structures of PNIPAM behave differently in all of these 2 × 40 metadynamics simulations resulting in distinct potential energy surfaces.

Although individual systems show a quite diverse behavior, the resulting averaged free energy surfaces above and below the LCST are in line with the experimentally observed behavior: below the LCST a random-coil conformation is thermodynamically favored, whereas above the LCST a globule conformation is thermodynamically favored.

As indicated in the Methods section, we also combined the metadynamics simulations with respect to their underlying probability distributions. The resulting combined free energy surfaces are depicted in Figure 5. Even though these two approaches to address the conformational sampling challenges rely on quite different assumptions, they result in strikingly similar free energy surfaces. Obviously, the individual barriers and relative free energies of the coil versus globule conformations vary due to different approaches. Still, the essentials remain the same: below the LCST the coil ensemble is thermodynamically favored, whereas above the LCST the globule ensemble dominates.

4. DISCUSSION

4.1. Lower Critical Solution Temperature. The conformation of PNIPAM can be characterized by the radius of gyration (ROG) and the solvent-accessible surface area (SASA). A random-coil conformation has a large ROG value around 1.7 nm, while a small ROG value around 1.0 nm suggests a globule conformation (Figure 2). Counting only hydrogen bonds is, in our view, not adequate to characterize the transition as the number of H-bonds may depend on the individual conformation of PNIPAM. Two very different structures may have the same number of H-bonds (Figure S7). The averaged ROG versus temperature plot (Figure 2) clearly shows a transition between 260 and 280 K. This force field LCST in our simulation is about 30−40 K lower compared to the experimental LCST.[1] However, the employed SPC/E water model has a melting point of 215 K.[89] In light of this huge shift in the water melting point, the shift in the coil−globule transition temperature is quite reasonable given the typical accuracy of force fields. The force field and water model combination was chosen based on literature recommendations,[76] where several force fields and water models were compared. The reported transition temperature of 320 K using the combination of OPLS-AA and SPC/E seemed to be in good agreement with the experimental LCST. The phase transition temperature difference between our simulations and published data is most likely related to the much longer simulation times applied here and slightly different force field parameters of OPLS2005. A recent study showed that a modification of the partial charges of the OPLS2005 force field might be used to tune the LCST.[66] Nevertheless, standard OPLS force fields as used in our study and by others are appropriate to describe the conformational transition associated with LCST.[54]

The LCST also depends on the tacticity,[21,23,24] the degree of polymerization,[89] and the concentration.[89] Meso-dyad-rich PNIPAMs exhibit higher hydrophobicity. An increase in meso dyad percentage will decrease the phase separation temperature and PNIPAM becomes insoluble once the meso dyad percentage exceeds 70%.[22] Although a fully isotactic PNIPAM, as used in this work, is a simplified model and, in an experiment, an isotactic PNIPAM chain is insoluble in water, conformational transitions were still observed. This may be attributed to the low degree of polymerization of our PNIPAM model and low concentration, as it is known that these two factors increase the phase separation temperature.[89] Due to the periodic conditions applied in the simulation box, the polymer concentration in our simulation is not infinitely diluted. Still, there is no interaction between the two polymers. It is worth noting that our results concerning the coil−globule transition are in line with those reported in refs 55 and 57, where the same isotactic PNIPAM models were used.

As mentioned in refs 54 55, and 64, the relaxation time of the PNIPAM is very long (>500 ns) and the convergence of the simulations is highly challenging. Our simulation time reaches 2 μs for systems with temperatures close to the force field LCST, and 1 μs was applied to systems at other temperatures to ensure adequate sampling. As depicted in Figure S4, while systems below or above the LCST stay in their respected thermodynamically favored conformational ensembles, systems around the force field LCST between 260 and 280 K cover a large conformational space visiting both random-coil and globule conformations. It is worth mentioning that we not only observed coil−globule transitions but also globule−coil backtransitions, which are only observed for very large time scales as reported previously.[55] This is reasonable as, at LCST, the difference in the free energy between the random-coil and globule states has to be zero, implying both states are equally populated.

4.2. Sampling of Conformational Phase Space. As PNIPAM does not exhibit a well-defined folding resulting in one (or a few) low-energy conformations, the conformational space of the globule is vast (Figure 3). Structures with different conformations may experience different transition mechanisms.[55] It is meaningless to study the free energy surface of a single PNIPAM structure as statistics are required. In our metadynamics simulations, we use the ROG as a collective variable, which is boosted to facilitate the globule−coil backtransitions. Even though we succeeded to enforce the transition, we also blocked out other globule structures having the same ROG. To overcome these issues and to have an implicit sampling of the phase space, 40 different starting structures were randomly picked from the ROG versus SASA subspace of the globule. For individual results of the metadynamics simulations, see Figure S6. While individual systems show considerable variations, the resulting averaged and combined free energy surfaces are remarkably stable towards leave-one-out cross-validation. This behavior indicates

DOI: 10.1021/acs.jpcb.9b06125
J. Phys. Chem. B 2019, 123, 8838−8847

that no single metadynamic simulation dominates the shape of the overall free energy surface. A considerable variation in free energy surfaces is expected since the transition mechanism varies for different starting structures.[55]

By starting metadynamics runs from globule conformations, the sampling in the random-coil conformational space might be insufficient, leading to an underestimation of the depth of the free energy well of the coil conformation. While we are well aware of these limitations and approximations, we still observe free energy surfaces that are in line with experimental findings.

4.3. Free Energy Surfaces above and below the LCST. Analysis of the resulting free energy surfaces above and below the LCST shows that, indeed, the OPLS2005 force field in combination with the SPC/E water model is consistent with the experimentally observed thermosensitive behavior, and the averaged and combined free energy surface curves reflect the thermoresponsive nature of the PNIPAM.

According to the averaged free energy surface, below the LCST, the random-coil ensemble is thermodynamically favored by $\Delta G_{C\rightarrow G}{}^{250} = 21 \pm 9$ kJ/mol (C, coil and G, globule). The energy barrier is not as accurately described as we have sparse sampling in this region. Besides, the expansion of PNIPAM in terms of the ROG, which is followed in each metadynamics simulation, may not necessarily coincide with the reaction coordinate of the expansion or swelling mechanism. Still, the obtained reaction barrier serves as an estimate. Below the LCST, at 250 K, the two distinct ensembles are separated by a globule → coil barrier $\Delta G^*_{G\rightarrow C}$ of 49 ± 14 kJ/mol. Such a high free energy barrier makes the spontaneous globule-to-random-coil phase transition highly unlikely to occur in any classic MD simulation even for time scales up to several microseconds. With the given barrier, we obtained a reaction rate constant of $k_{G\rightarrow C} = 301\ s^{-1}$, corresponding to a half-life of $t_{1/2\ G\rightarrow C} = 2300\ \mu s$ and an equilibrium constant of $K_{equ\ C\rightarrow G} = 4.1 \times 10^{-5}$. As the half-life is several orders of magnitude longer than our simulation time, this explains why the globule−coil transition has never been observed in the low-temperature regime of our simulations, and the 30-mer is kinetically trapped in a globule conformation. Above the LCST, at 300 K, the two conformational ensembles are separated by a coil → globule barrier $\Delta G^*_{C\rightarrow G}$ of only 17 ± 10 kJ/mol and the free energy difference $\Delta G_{G\rightarrow C}{}^{300}$ is 21 ± 8 kJ/mol in favor of the globule. For this barrier, the reaction rate constant is $k_{C\rightarrow G} = 6.86 \times 10^9\ s^{-1}$ and the half-life is $t_{1/2\ C\rightarrow G} = 1 \times 10^{-4}\ \mu s$, whereas the equilibrium constant $K_{equ\ G\rightarrow C} = 2.2 \times 10^{-4}$. This obtained half-life is significantly shorter than the simulated time scale and explains the observation of spontaneous coil−globule transitions in almost all high-temperature simulations.

For the globule−coil backtransition at 250 K, the globule → coil barrier $\Delta G^*_{G\rightarrow C}$ is 49 ± 14 kJ/mol which is within the margin of error of the corresponding globule → coil barrier at 300 K of $\Delta G^*_{G\rightarrow C} = 38 \pm 9$ kJ/mol. However, the coil → globule barrier at 250 K is $\Delta G^*_{C\rightarrow G} = 70 \pm 14$ kJ/mol, which is much higher than the corresponding coil → globule barrier at 300 K of $\Delta G^*_{C\rightarrow G} = 17 \pm 10$ kJ/mol. This may be as a result of the neatly arranged water molecules in the first hydration layer of the random-coil structure at a lower temperature. Presumably, more favorable solute−solvent interaction might stabilize the random-coil structure, resulting in an increase of the coil → globule barrier at 250 K.

On the other hand, in the combined free energy surface at 250 K, we get a free energy difference $\Delta G_{C\rightarrow G}{}^{250} = 5$ kJ/mol in favor of the random-coil and a globule → coil barrier $\Delta G^*_{G\rightarrow C} = 41$ kJ/mol. Thus, we calculated a reaction rate constant of $k_{G\rightarrow C} = 1.2 \times 10^4\ s^{-1}$, corresponding to a half-life of $t_{1/2\ G\rightarrow C} = 59\ \mu s$ and an equilibrium constant of $K_{equ\ C\rightarrow G} = 0.1$. At 300 K, the free energy difference is $\Delta G_{G\rightarrow C}{}^{300}$ is 41 kJ/mol in favor of the globule and the coil → globule barrier $\Delta G^*_{C\rightarrow G}$ is 30 kJ/mol. These values correspond to a reaction rate constant of $k_{C\rightarrow G} = 4.4 \times 10^7\ s^{-1}$, a half-life of $t_{1/2\ C\rightarrow G} = 158$ ns, and an equilibrium constant of $K_{equ\ G\rightarrow C} = 7.8 \times 10^{-8}$.

The results shown in Figure 5 agree with the behavior observed in the free simulations and are fully consistent with Figure 4. Even more, the equilibrium constants and especially the reaction rates we calculated from these estimated free energy curves are in a reasonable order of magnitude. Also, according to these results, it is not expected to see a globule−coil transition at low temperatures in a time scale, which is reachable with unbiased molecular dynamics simulations. Furthermore, an expected time scale for the coil−globule transition of a few nanoseconds at 300 K is consistent with our own results and with previously published data.[51,56] As both approaches to estimate the free energy surfaces above and below the LCST resulted in remarkably similar results, we are confident that sampling and convergences issues are handled appropriately.

Lastly, it is worth noting that the collapse of PNIPAM was observed for a single 30-mer chain in the water where there were no intermolecular polymer−polymer interactions. While this does not seem to be a realistic system at first glance, intricate single-molecule force spectroscopy investigations experimentally confirmed a collapse for a single PNIPAM molecule.[69] This finding indicates that cooperative effects, though they may play an essential role in the aggregation process, are not the dominant factors contributing to the thermosensitive behavior of PNIPAM.

5. CONCLUSIONS

We determined the phase transition of an isotactic 30-mer of PNIPAM and found an LCST between 260 and 280 K for the OPLS2005 force field in combination with the SPC/E water. The two conformational ensembles, the globule and the random-coil, can be very well distinguished in 2D ROG and SASA phase space. Discrimination of the two states by the number of hydrogen bonds is, in our view, not adequate because of the diverse globule space, where structures at a given radius of gyration differ in their number of hydrogen bonds. We showed that a vast sampling of the diverse globule phase space is required to obtain reliable estimates. For the first time, free energy surfaces above and below the LCST were presented, which show that the OPLS2005 force field agrees with the experimentally observed thermosensitive behavior. While the standard OPLS2005 force field required long simulation times, it correctly predicted the random-coil conformational ensemble to be the thermodynamic minimum below the LCST, whereas above the LCST it is the globule ensemble that represents the global energy minimum. The calculated half-life of the barriers explains why a globule−coil transition is not observed in the applied simulation time scale.

Despite the fact that fully isotactic PNIPAM is experimentally insoluble in water, our isotactic 30-mer single PNIPAM in water simulations still showed conformational transitions associated with the LCST. The reported results may pave the way for further investigations of the hydrophobicity and hydrophilicity of the structural ensembles and an atomistic

DOI: 10.1021/acs.jpcb.9b06125
J. Phys. Chem. B 2019, 123, 8838−8847

understanding of the transition mechanism. However, variations in tacticity may impact the calculated LCST, thus, further investigation of PNIPAM models with different meso dyad percentages is required to access this effect and to further corroborate the findings of this study. Multipolymer chain aggregation may be an extension of this work to access the effect of cooperativity in this process thoroughly. A sound characterization both experimentally and computationally is a prerequisite for using and tuning thermosensitive polymers as drug delivery agents.

■ ASSOCIATED CONTENT

Supporting Information

The Supporting Information is available free of charge on the ACS Publications website at DOI: 10.1021/acs.jpcb.9b06125.

Details about simulation time used in each temperature, graphical representations of conformational space of ROG vs SASA and ROG vs end to end distance for each temperature, ROG vs time plot for phase transition simulations and metadynamic simulations, as well as plots of hydrogen bond number vs ROG and SASA (PDF)

■ AUTHOR INFORMATION

Corresponding Author

*E-mail: Klaus.Liedl@uibk.ac.at.

ORCID

Maren Podewitz: 0000-0001-7256-1219
Johannes R. Loeffler: 0000-0002-5724-655X
Michael Schauperl: 0000-0001-5648-8170
Klaus R. Liedl: 0000-0002-0985-2299

Present Address

†Skaggs School of Pharmacy and Pharmaceutical Sciences, University of California, San Diego, California 92093, United States (M.S.).

Author Contributions

‡M.P. and Y.W. contributed equally to this work.

Notes

The authors declare no competing financial interest.

■ ACKNOWLEDGMENTS

The computational results presented have been achieved using the HPC infrastructure LEO of the University of Innsbruck and the Vienna Scientific Cluster (VSC). Financial support by the European Commission and by Marie Curie Actions for Ph.D. fellowship to Y.W. (contract agreement number 289454) and by the European Union's Horizon 2020 research and innovation programme to P.K.Q. under grant agreement number 764958 and by the Austrian Science Fund (FWF) (project: P30565) is acknowledged. M.P. and M.S. would like to thank the FWF for their postdoctoral fellowships (M.P.: grant number M 2005-NBL; M.S.: grant number J-4150).

■ REFERENCES

(1) Heskins, M.; Guillet, J. E. Solution Properties of Poly(*N*-isopropylacrylamide). *J. Macromol. Sci., Chem.* **1968**, *2*, 1441−1455.

(2) Fujishige, S.; Kubota, K.; Ando, I. Phase Transition of Aqueous Solutions of Poly(N-Isopropylacrylamide) and Poly(N-Isopropylmethacrylamide). *J. Phys. Chem. A* **1989**, *93*, 3311−3313.

(3) Bromberg, L. E.; Ron, E. S. Temperature-Responsive Gels and Thermogelling Polymer Matrices for Protein and Peptide Delivery. *Adv. Drug Delivery Rev.* **1998**, *31*, 197−221.

(4) Li, Y.; Wang, Y.; Huang, G.; Gao, J. Cooperativity Principles in Self-Assembled Nanomedicine. *Chem. Rev.* **2018**, *118*, 5359−5391.

(5) Ferreira, N.; Ferreira, L.; Cardoso, V.; Boni, F.; Souza, A.; Gremião, M. Recent Advances in Smart Hydrogels for Biomedical Applications: From Self-Assembly to Functional Approaches. *Eur. Polym. J.* **2018**, *99*, 117−133.

(6) Nagase, K.; Yamato, M.; Kanazawa, H.; Okano, T. Poly(N-Isopropylacrylamide)-Based Thermoresponsive Surfaces Provide New Types of Biomedical Applications. *Biomaterials* **2018**, *153*, 27−48.

(7) Lanzalaco, S.; Armelin, E. Poly(N-Isopropylacrylamide) and Copolymers: A Review on Recent Progresses in Biomedical Applications. *Gels* **2017**, *3*, No. 36.

(8) Vanparijs, N.; Nuhn, L.; De Geest, B. G. Transiently Thermoresponsive Polymers and Their Applications in Biomedicine. *Chem. Soc. Rev.* **2017**, *46*, 1193−1239.

(9) Wei, M.; Gao, Y.; Li, X.; Serpe, M. J. Stimuli-Responsive Polymers and Their Applications. *Polym. Chem.* **2017**, *8*, 127−143.

(10) Mano, J. F. Stimuli-Responsive Polymeric Systems for Biomedical Applications. *Adv. Eng. Mater.* **2008**, *10*, 515−527.

(11) Karg, M.; Pich, A.; Hellweg, T.; Hoare, T.; Lyon, L. A.; Crassous, J. J.; Suzuki, D.; Gumerov, R. A.; Schneider, S.; Potemkin, I. I.; et al. Nanogels and Microgels: From Model Colloids to Applications, Recent Developments, and Future Trends. *Langmuir* **2019**, *35*, 6231−6255.

(12) Moghadam, S.; Larson, R. G. Assessing the Efficacy of Poly(N-Isopropylacrylamide) for Drug Delivery Applications Using Molecular Dynamics Simulations. *Mol. Pharm.* **2017**, *14*, 478−491.

(13) Stuart, M. A. C.; Huck, W. T. S.; Genzer, J.; Müller, M.; Ober, C.; Stamm, M.; Sukhorukov, G. B.; Szleifer, I.; Tsukruk, V. V.; Urban, M.; et al. Emerging Applications of Stimuli-Responsive Polymer Materials. *Nat. Mater.* **2010**, *9*, 101−113.

(14) Fu, X.; Hosta-Rigau, L.; Chandrawati, R.; Cui, J. Multi-Stimuli-Responsive Polymer Particles, Films, and Hydrogels for Drug Delivery. *Chem* **2018**, 2084−2107.

(15) Qiu, Y.; Park, K. Environment-Sensitive Hydrogels for Drug Delivery. *Adv. Drug Delivery Rev.* **2001**, *53*, 321−339.

(16) Schmaljohann, D. Thermo- and pH-Responsive Polymers in Drug Delivery. *Adv. Drug Delivery Rev.* **2006**, *58*, 1655−1670.

(17) Zuo, Y.; Gou, Z.; Zhang, Y.; Yang, T.; Lin, W. Thermally Responsive Materials for Bioimaging. *Chem.: Asian J.* **2019**, *14*, 67−75.

(18) Schild, H. G.; Tirrell, D. A. Microcalorimetric Detection of Lower Critical Solution Temperatures in Aqueous Polymer-Solutions. *J. Phys. Chem. A* **1990**, *94*, 4352−4356.

(19) Tucker, A. K.; Stevens, M. J. Study of the Polymer Length Dependence of the Single Chain Transition Temperature in Syndiotactic Poly(N-Isopropylacrylamide) Oligomers in Water. *Macromolecules* **2012**, *45*, 6697−6703.

(20) Barker, I. C.; Cowie, J. M. G.; Huckerby, T. N.; Shaw, D. A.; Soutar, I.; Swanson, L. Studies of the "Smart" Thermoresponsive Behavior of Copolymers of N-Isopropylacrylamide and N,N-Dimethylacrylamide in Dilute Aqueous Solution. *Macromolecules* **2003**, *36*, 7765−7770.

(21) de Oliveira, T. E.; Mukherji, D.; Kremer, K.; Netz, P. A. Effects of Stereochemistry and Copolymerization on the LCST of PNIPAm. *J. Chem. Phys.* **2017**, *146*, No. 034904.

(22) Ray, B.; Okamoto, Y.; Kamigaito, M.; Sawamoto, M.; Seno, K.; Kanaoka, S.; Aoshima, S. Effect of Tacticity of Poly(N-Isopropylacrylamide) on the Phase Separation Temperature of Its Aqueous Solutions. *Polym. J.* **2005**, *37*, 234−237.

(23) Chiessi, E.; Paradossi, G. Influence of Tacticity on Hydrophobicity of Poly(N-Isopropylacrylamide): A Single Chain Molecular Dynamics Simulation Study. *J. Phys. Chem. B* **2016**, *120*, 3765−3776.

(24) Paradossi, G.; Chiessi, E. Tacticity-Dependent Interchain Interactions of Poly(N-Isopropylacrylamide) in Water: Toward the

DOI: 10.1021/acs.jpcb.9b06125
J. Phys. Chem. B 2019, 123, 8838−8847

Molecular Dynamics Simulation of a Thermoresponsive Microgel. *Gels* **2017**, *3*, No. 13.
(25) Bruce, E. E.; Bui, P. T.; Rogers, B. A.; Cremer, P. S.; van der Vegt, N. F. A. Nonadditive Ion Effects Drive Both Collapse and Swelling of Thermoresponsive Polymers in Water. *J. Am. Chem. Soc.* **2019**, *141*, 6609−6616.
(26) Pérez-Fuentes, L.; Drummond, C.; Faraudo, J.; Bastos-González, D. Anions Make the Difference: Insights from the Interaction of Big Cations and Anions with Poly(N-Isopropylacrylamide) Chains and Microgels. *Soft Matter* **2015**, *11*, 5077−5086.
(27) Rodríguez-Ropero, F.; van der Vegt, N. F. A. Direct Osmolyte-Macromolecule Interactions Confer Entropic Stability to Folded States. *J. Phys. Chem. B* **2014**, *118*, 7327−7334.
(28) Rodríguez-Ropero, F.; van der Vegt, N. F. A. On the Urea Induced Hydrophobic Collapse of a Water Soluble Polymer. *Phys. Chem. Chem. Phys.* **2015**, *17*, 8491−8498.
(29) Zhu, P. W.; Chen, L. G. Effects of Cosolvent Partitioning on Conformational Transitions and Chain Flexibility of Thermoresponsive Microgels. *Phys. Rev. E* **2019**, *99*, No. 022501.
(30) Kyriakos, K.; Philipp, M.; Lin, C.-H.; Dyakonova, M.; Vishnevetskaya, N.; Grillo, I.; Zaccone, A.; Miasnikova, A.; Laschewsky, A.; Müller-Buschbaum, P.; et al. Quantifying the Interactions in the Aggregation of Thermoresponsive Polymers: The Effect of Cononsolvency. *Macromol. Rapid Commun.* **2016**, *37*, 420−425.
(31) Bischofberger, I.; Calzolari, D. C. E.; Trappe, V. Co-Nonsolvency of PNiPAM at the Transition between Solvation Mechanisms. *Soft Matter* **2014**, *10*, 8288−8295.
(32) Bischofberger, I.; Calzolari, D. C. E.; De Los Rios, P.; Jelezarov, I.; Trappe, V. Hydrophobic Hydration of Poly-N-Isopropyl Acrylamide: A Matter of the Mean Energetic State of Water. *Sci. Rep.* **2014**, *4*, No. 4377.
(33) Tanaka, F.; Koga, T.; Winnik, F. M. Temperature-Responsive Polymers in Mixed Solvents: Competitive Hydrogen Bonds Cause Cononsolvency. *Phys. Rev. Lett.* **2008**, *101*, No. 028302.
(34) Schild, H. G.; Muthukumar, M.; Tirrell, D. A. Cononsolvency in Mixed Aqueous-Solutions of Poly(N-Isopropylacrylamide). *Macromolecules* **1991**, *24*, 948−952.
(35) Mukherji, D.; Wagner, M.; Watson, M. D.; Winzen, S.; de Oliveira, T. E.; Marques, C. M.; Kremer, K. Relating Side Chain Organization of PNIPAm with Its Conformation in Aqueous Methanol. *Soft Matter* **2016**, *12*, 7995−8003.
(36) Mochizuki, K.; Sumi, T.; Koga, K. Driving Forces for the Pressure-Induced Aggregation of Poly(N-Isopropylacrylamide) in Water. *Phys. Chem. Chem. Phys.* **2016**, *18*, 4697−4703.
(37) Kubota, K.; Fujishige, S.; Ando, I. Solution Properties of Poly(N-Isopropylacrylamide) in Water. *Polym. J.* **1990**, *22*, 15−20.
(38) Ilmain, F.; Tanaka, T.; Kokufuta, E. Volume Transition in a Gel Driven by Hydrogen-Bonding. *Nature* **1991**, *349*, 400−401.
(39) Cho, E. C.; Lee, J.; Cho, K. Role of Bound Water and Hydrophobic Interaction in Phase Transition of Poly(N-Isopropylacrylamide) Aqueous Solution. *Macromolecules* **2003**, *36*, 9929−9934.
(40) Ahmed, Z.; Gooding, E. A.; Pimenov, K. V.; Wang, L.; Asher, S. A. UV Resonance Raman Determination of Molecular Mechanism of Poly(N-Isopropylacrylamide) Volume Phase Transition. *J. Phys. Chem. B* **2009**, *113*, 4248−4256.
(41) Juurinen, I.; Galambosi, S.; Anghelescu-Hakala, A. G.; Koskelo, J.; Honkimaki, V.; Hamalainen, K.; Huotari, S.; Hakala, M. Molecular-Level Changes of Aqueous Poly(N-Isopropylacrylamide) in Phase Transition. *J. Phys. Chem. B* **2014**, *118*, 5518−5523.
(42) Shiraga, K.; Naito, H.; Suzuki, T.; Kondo, N.; Ogawa, Y. Hydration and Hydrogen Bond Network of Water During the Coil-to-Globule Transition in Poly(N-Isopropylacrylamide) Aqueous Solution at Cloud Point Temperature. *J. Phys. Chem. B* **2015**, *119*, 5576−5587.
(43) Futscher, M. H.; Philipp, M.; Müller-Buschbaum, P.; Schulte, A. The Role of Backbone Hydration of Poly(N-Isopropyl Acrylamide) across the Volume Phase Transition Compared to Its Monomer. *Sci. Rep.* **2017**, *7*, No. 17012.
(44) Parrish, E.; Seeger, S. C.; Composto, R. J. Temperature-Dependent Nanoparticle Dynamics in Poly(N-Isopropylacrylamide) Gels. *Macromolecules* **2018**, *51*, 3597−3607.
(45) Lopez, C. G.; Scotti, A.; Brugnoni, M.; Richtering, W. The Swelling of Poly(Isopropylacrylamide) near the θ Temperature: A Comparison between Linear and Cross-Linked Chains. *Macromol. Chem. Phys.* **2019**, *220*, No. 1800421.
(46) Keidel, R.; Ghavami, A.; Lugo, D. M.; Lotze, G.; Virtanen, O.; Beumers, P.; Pedersen, J. S.; Bardow, A.; Winkler, R. G.; Richtering, W. Time-Resolved Structural Evolution During the Collapse of Responsive Hydrogels: The Microgel-to-Particle Transition. *Sci. Adv.* **2018**, *4*, No. eaao7086.
(47) Virtanen, O. L. J.; Kather, M.; Meyer-Kirschner, J.; Melle, A.; Radulescu, A.; Viell, J. D.; Mitsos, A.; Pich, A.; Richtering, W. Direct Monitoring of Microgel Formation During Precipitation Polymerization of N-Isopropylacrylamide Using in Situ SANS. *ACS Omega* **2019**, *4*, 3690−3699.
(48) Philipp, M.; Kyriakos, K.; Silvi, L.; Lohstroh, W.; Petry, W.; Krüger, J. K.; Papadakis, C. M.; Müller-Buschbaum, P. From Molecular Dehydration to Excess Volumes of Phase-Separating PNIPAM Solutions. *J. Phys. Chem. B* **2014**, *118*, 4253−4260.
(49) Lai, H.; Wu, P. A Infrared Spectroscopic Study on the Mechanism of Temperature-Induced Phase Transition of Concentrated Aqueous Solutions of Poly(N-Isopropylacrylamide) and N-Isopropylpropionamide. *Polymer* **2010**, *51*, 1404−1412.
(50) Deshmukh, S. A.; Sankaranarayanan, S. K. R. S.; Mancini, D. C. Vibrational Spectra of Proximal Water in a Thermo-Sensitive Polymer Undergoing Conformational Transition across the Lower Critical Solution Temperature. *J. Phys. Chem. B* **2012**, *116*, 5501−5515.
(51) Deshmukh, S. A.; Sankaranarayanan, S. K. R. S.; Suthar, K.; Mancini, D. C. Role of Solvation Dynamics and Local Ordering of Water in Inducing Conformational Transitions in Poly(N-Isopropylacrylamide) Oligomers through the LCST. *J. Phys. Chem. B* **2012**, *116*, 2651−2663.
(52) Deshmukh, S. A.; Kamath, G.; Suthar, K. J.; Mancini, D. C.; Sankaranarayanan, S. K. R. S. Non-Equilibrium Effects Evidenced by Vibrational Spectra During the Coil-to-Globule Transition in Poly(N-Isopropylacrylamide) Subjected to an Ultrafast Heating-Cooling Cycle. *Soft Matter* **2014**, *10*, 1462−1480.
(53) Abbott, L. J.; Tucker, A. K.; Stevens, M. J. Single Chain Structure of a Poly(N-Isopropylacrylamide) Surfactant in Water. *J. Phys. Chem. B* **2015**, *119*, 3837−3845.
(54) Botan, V.; Ustach, V.; Faller, R.; Leonhard, K. Direct Phase Equilibrium Simulations of NIPAM Oligomers in Water. *J. Phys. Chem. B* **2016**, *120*, 3434−3440.
(55) Kang, Y.; Joo, H.; Kim, J. S. Collapse-Swelling Transitions of a Thermoresponsive, Single Poly(N-Isopropylacrylamide) Chain in Water. *J. Phys. Chem. B* **2016**, *120*, 13184−13192.
(56) Singh, R.; Deshmukh, S. A.; Kamath, G.; Sankaranarayanan, S. K. R. S.; Balasubramanian, G. Controlling the Aqueous Solubility of PNIPAM with Hydrophobic Molecular Units. *Comput. Mater. Sci.* **2017**, *126*, 191−203.
(57) Adroher-Benítez, I.; Moncho-Jorda, A.; Odriozola, G. Conformation Change of an Isotactic Poly(N-Isopropylacrylamide) Membrane: Molecular Dynamics. *J. Chem. Phys.* **2017**, *146*, No. 194905.
(58) Kanduč, M.; Kim, W. K.; Roa, R.; Dzubiella, J. Selective Molecular Transport in Thermoresponsive Polymer Membranes: Role of Nanoscale Hydration and Fluctuations. *Macromolecules* **2018**, *51*, 4853−4864.
(59) Bejagam, K. K.; An, Y. X.; Singh, S.; Deshmukh, S. A. Machine-Learning Enabled New Insights into the Coil-to-Globule Transition of Thermosensitive Polymers Using a Coarse-Grained Model. *J. Phys. Chem. Lett.* **2018**, *9*, 6480−6488.
(60) Tavagnacco, L.; Zaccarelli, E.; Chiessi, E. On the Molecular Origin of the Cooperative Coil-to-Globule Transition of Poly(N-Isopropylacrylamide) in Water. *Phys. Chem. Chem. Phys.* **2018**, *20*, 9997−10010.

DOI: 10.1021/acs.jpcb.9b06125
J. Phys. Chem. B 2019, 123, 8838−8847

(61) Tavagnacco, L.; Chiessi, E.; Zanatta, M.; Orecchini, A.; Zaccarelli, E. Water-Polymer Coupling Induces a Dynamical Transition in Microgels. *J. Phys. Chem. Lett.* **2019**, *10*, 870−876.
(62) Camerin, F.; Gnan, N.; Rovigatti, L.; Zaccarelli, E. Modelling Realistic Microgels in an Explicit Solvent. *Sci. Rep.* **2018**, *8*, No. 14426.
(63) van der Vegt, N. F. A.; Nayar, D. The Hydrophobic Effect and the Role of Cosolvents. *J. Phys. Chem. B* **2017**, *121*, 9986−9998.
(64) García, E. J.; Hasse, H. Studying Equilibria of Polymers in Solution by Direct Molecular Dynamics Simulations: Poly(N-Isopropylacrylamide) in Water as a Test Case. *Eur. Phys. J.: Spec. Top.* **2019**, *227*, 1547−1558.
(65) Dalgicdir, C.; Rodriguez-Ropero, F.; van der Vegt, N. F. A. Computational Calorimetry of PNIPAM Cononsolvency in Water/Methanol Mixtures. *J. Phys. Chem. B* **2017**, *121*, 7741−7748.
(66) Dalgicdir, C.; van der Vegt, N. F. A. Improved Temperature Behavior of PNIPAM in Water with a Modified OPLS Model. *J. Phys. Chem. B* **2019**, *123*, 3875−3883.
(67) Kamath, G.; Deshmukh, S. A.; Baker, G. A.; Mancini, D. C.; Sankaranarayanan, S. K. R. S. Thermodynamic Considerations for Solubility and Conformational Transitions of Poly-N-Isopropyl-Acrylamide. *Phys. Chem. Chem. Phys.* **2013**, *15*, 12667−12673.
(68) Nayar, D.; Folberth, A.; van der Vegt, N. F. Molecular Origin of Urea Driven Hydrophobic Polymer Collapse and Unfolding Depending on Side Chain Chemistry. *Phys. Chem. Chem. Phys.* **2017**, *19*, 18156−18161.
(69) Pang, X. C.; Cui, S. X. Single-Chain Mechanics of Poly(N,N-Diethylacrylamide) and Poly(N-Isopropylacrylamide): Comparative Study Reveals the Effect of Hydrogen Bond Donors. *Langmuir* **2013**, *29*, 12176−12182.
(70) Wang, X.; Wu, C. Light-Scattering Study of Coil-to-Globule Transition of a Poly(N-Isopropylacrylamide) Chain in Deuterated Water. *Macromolecules* **1999**, *32*, 4299−4301.
(71) Virtanen, J.; Holappa, S.; Lemmetyinen, H.; Tenhu, H. Aggregation in Aqueous Poly(N-Isopropylacrylamide)-Block-Poly-(Ethylene Oxide) Solutions Studied by Fluorescence Spectroscopy and Light Scattering. *Macromolecules* **2002**, *35*, 4763−4769.
(72) Kaminski, G. A.; Friesner, R. A.; Tirado-Rives, J.; Jorgensen, W. L. Evaluation and Reparametrization of the OPLS-AA Force Field for Proteins Via Comparison with Accurate Quantum Chemical Calculations on Peptides. *J. Phys. Chem. B* **2001**, *105*, 6474−6487.
(73) Jorgensen, W. L.; Maxwell, D. S.; Tirado-Rives, J. Development and Testing of the OPLS All-Atom Force Field on Conformational Energetics and Properties of Organic Liquids. *J. Am. Chem. Soc.* **1996**, *118*, 11225−11236.
(74) *Schrödinger Release 2018-1: Maestro*; Schrödinger, LLC: New York, NY, 2018.
(75) Berendsen, H. J. C.; Grigera, J. R.; Straatsma, T. P. The Missing Term in Effective Pair Potentials. *J. Phys. Chem. A* **1987**, *91*, 6269−6271.
(76) Walter, J.; Ermatchkov, V.; Vrabec, J.; Hasse, H. Molecular Dynamics and Experimental Study of Conformation Change of Poly(N-Isopropylacrylamide) Hydrogels in Water. *Fluid Phase Equilib.* **2010**, *296*, 164−172.
(77) Berendsen, H. J. C.; Vanderspoel, D.; Vandrunen, R. Gromacs - a Message-Passing Parallel Molecular-Dynamics Implementation. *Comput. Phys. Commun.* **1995**, *91*, 43−56.
(78) Hess, B.; Kutzner, C.; van der Spoel, D.; Lindahl, E. GROMACS 4: Algorithms for Highly Efficient, Load-Balanced, and Scalable Molecular Simulation. *J. Chem. Theory Comput.* **2008**, *4*, 435−447.
(79) Hess, B.; Bekker, H.; Berendsen, H. J.; Fraaije, J. G. Lincs: A Linear Constraint Solver for Molecular Simulations. *J. Comput. Chem.* **1997**, *18*, 1463−1472.
(80) Essmann, U.; Perera, L.; Berkowitz, M. L.; Darden, T.; Lee, H.; Pedersen, L. G. A Smooth Particle Mesh Ewald Method. *J. Chem. Phys.* **1995**, *103*, 8577−8593.
(81) Bussi, G.; Donadio, D.; Parrinello, M. Canonical Sampling through Velocity Rescaling. *J. Chem. Phys.* **2007**, *126*, No. 014101.
(82) Parrinello, M.; Rahman, A. Polymorphic Transitions in Single-Crystals - a New Molecular-Dynamics Method. *J. Appl. Phys.* **1981**, *52*, 7182−7190.
(83) Eisenhaber, F.; Lijnzaad, P.; Argos, P.; Sander, C.; Scharf, M. The Double Cubic Lattice Method: Efficient Approaches to Numerical Integration of Surface Area and Volume and to Dot Surface Contouring of Molecular Assemblies. *J. Comput. Chem.* **1995**, *16*, 273−284.
(84) Laio, A.; Parrinello, M. Escaping Free-Energy Minima. *Proc. Natl. Acad. Sci. U.S.A.* **2002**, *99*, 12562−12566.
(85) Barducci, A.; Bussi, G.; Parrinello, M. Well-Tempered Metadynamics: A Smoothly Converging and Tunable Free-Energy Method. *Phys. Rev. Lett.* **2008**, *100*, No. 020603.
(86) Bonomi, M.; Branduardi, D.; Bussi, G.; Camilloni, C.; Provasi, D.; Raiteri, P.; Donadio, D.; Marinelli, F.; Pietrucci, F.; Broglia, R. A.; Parrinello, M. PLUMED: A Portable Plugin for Free-Energy Calculations with Molecular Dynamics. *Comput. Phys. Commun.* **2009**, *180*, 1961−1972.
(87) Bonomi, M.; Barducci, A.; Parrinello, M. Reconstructing the Equilibrium Boltzmann Distribution from Well-Tempered Metadynamics. *J. Comput. Chem.* **2009**, *30*, 1615−1621.
(88) Tiwary, P.; Parrinello, M. A Time-Independent Free Energy Estimator for Metadynamics. *J. Phys. Chem. B* **2015**, *119*, 736−742.
(89) Pamies, R.; Zhu, K.; Kjøniksen, A.-L.; Nyström, B. Thermal Response of Low Molecular Weight Poly-(N-Isopropylacrylamide) Polymers in Aqueous Solution. *Polym. Bull.* **2009**, *62*, 487−502.

DOI: 10.1021/acs.jpcb.9b06125
J. Phys. Chem. B 2019, 123, 8838−8847